Documentation of open-source MFIX-variable particle density software for reacting gas-particle flows*

Q. Xue
qlxue@iastate.edu

Department of Chemical and Biological Engineering, Iowa State University, Ames, IA 50011, USA

R. O. Fox
rofox@iastate.edu

Department of Chemical and Biological Engineering, Iowa State University, Ames, IA 50011, USA

January 31, 2013

*Please refer to this document as: Q. Xue, R. O. Fox, Documentation of open-source MFIX-variable particle density software for reacting gas-solids flows, From URL https://mfix.netl.doe.gov/documentation/variable-particle-density-doc-2013-1.pdf

Contents

1 Introduction

Understanding the transport of heat and mass in multiphase flows, and accurate modeling of related phenomena is critical to the efficient design and scale-up of energy and chemical process equipment. Polydisperse gas-solid flows, composed of particles with varying characteristics including mass, volume, shape, surface roughness, with or without the influence of carrier fluids, are important in energy processes such as coal and biomass gasification.

Naturally, the reacting particles in energy systems such as gasifiers have a varying solids density due to volatilization of lighter components and chemical reactions. Because the solid density is a critical parameter in determining particle segregation, product distribution, particle residence time, and char elutriation, it is critical to include variable solid density in the MFIX model for biomass/coal gasification. This document first concisely describes the implementation of a continuous variable-density model, valid for arbitrary solid density descriptions, in MFIX (Multiphase Flow with Interphase eXchanges) from the National Energy Technology Laboratory (NETL) (Syamlal et al., 1993; Syamlal, 1998) for polydisperse reacting gas-particle flows. Then, a tutorial for running the test case is provided. Details can be found in the work by Xue et al. (2011, 2012); Xue and Fox (2012, 2013).

2 Polydisperse reactor multi-fluid CFD model

In the multi-fluid CFD model, the gas and solid phases are treated as inter-penetrating continua in an Eulerian framework. The gas is considered as the primary phase, whereas the solid phases are considered as secondary or dispersed phases. Each solid phase is distinguished by its physical properties (diameter, density, etc.) or through its thermal properties (reactive or inert particles). Multiple solid phases allow for describing phenomena such as segregation and elutriation. The primary and dispersed phases are linked by tracking the phase volume fractions in a finite-volume frame. These volume fractions are assumed to be functions of space and time. By definition, the volume fractions of all of the phases must sum to unity:

$$\epsilon_g + \sum_{m=1}^{M} \epsilon_{sm} = 1 \tag{1}$$

where ϵ_g is the gas volume fraction, ϵ_{sm} is the volume fraction of m^{th} dispersed phase, and M is the total number of dispersed phases. The multi-fluid CFD model for gas-solid flow is described briefly below. More details can be found elsewhere (Syamlal et al., 1993). The emphasis is placed on the mass, momentum, and heat transfer terms due to gas-solid surface chemistry.

2.1 Gas phase

The gas phase is formulated through a set of conservation equations for mass, momentum, and energy. The continuity equation for the gas phase is

$$\frac{\partial \epsilon_g \rho_g}{\partial t} + \nabla \cdot (\epsilon_g \rho_g \vec{\mathbf{u}}_g) = R_g \tag{2}$$

where ρ_g is the density of the gas, and $\vec{\mathbf{u}}_g$ is the velocity of gas, and R_g are the interphase mass transfer terms from the solid phase due to surface chemistry at the gas-solid interface or physical processes (such as evaporation). For our kinetic model, $R_g = \sum_{n=1}^{N} R_{gn}$, where the expressions for R_{gn} are listed in Eq. (29).

The momentum equation for the gas phase is

$$\frac{\partial \epsilon_g \rho_g \vec{\mathbf{u}}_g}{\partial t} + \nabla \cdot (\epsilon_g \rho_g \vec{\mathbf{u}}_g \vec{\mathbf{u}}_g) = \nabla \cdot \bar{\bar{\mathbf{S}}}_g + \sum_{m=1}^{M} \vec{\mathbf{I}}_{gm} + \epsilon_g \rho_g \vec{\mathbf{g}} \tag{3}$$

where $\bar{\bar{\mathbf{S}}}_g$ is the second-order stress tensor for the gas, $\vec{\mathbf{I}}_{gm}$ is an interaction force representing the momentum transfer between the gas and the m^{th} solid phase, and $\vec{\mathbf{g}}$ is the gravity vector. The momentum exchange, included in $\vec{\mathbf{I}}_{gm}$, due to mass transfer from solid phase m to the gas phase is described as

$$\sum_{n=1}^{N} R_{smn}[\xi_{gm}\vec{\mathbf{u}}_{sm} + (1-\xi_{gm})\vec{\mathbf{u}}_g] \qquad \text{with } \xi_{gm} = \begin{cases} 0 & \text{if } \sum_{n=1}^{N} R_{smn} < 0, \\ 1 & \text{if } \sum_{n=1}^{N} R_{smn} \geq 0. \end{cases} \tag{4}$$

The energy equation for the gas phase in terms of the gas phase temperature is

$$\epsilon_g \rho_g C_{pg} \left(\frac{\partial T_g}{\partial t} + \vec{\mathbf{u}}_g \cdot \nabla T_g \right) = \nabla \cdot \vec{\mathbf{q}}_g - \sum_{m=1}^{M} H_{gm} - \Delta H_{rg} + H_{wall}(T_{wall} - T_g) \tag{5}$$

where $\vec{\mathbf{q}}_g$ is the gas-phase conductive heat flux, H_{gm} describes fluid-solids interphase heat transfer between the gas and m^{th} solids, and ΔH_{rg} is the heat of reaction in the gas phase. The last term accounts for the heat loss to the wall.

2.2 Solid phases

The solid phases are formulated through a set of conservation equations for mass, momentum, and energy. The continuity equation for solid phase m is

$$\frac{\partial \epsilon_{sm}\rho_{sm}}{\partial t} + \nabla \cdot (\epsilon_{sm}\rho_{sm}\vec{\mathbf{u}}_{sm}) = R_{sm} \tag{6}$$

where ρ_{sm} is the density, $\vec{\mathbf{u}}_{sm}$ is the velocity of solid phase m, and $R_{sm} = \sum_{n=1}^{N} R_{smn}$ due to gas-solid surface chemistry. The expressions for R_{smn} are listed in Eq. (30). Due to conservation of mass, $\sum_{m=1}^{M} R_{sm} + R_g = 0$.

The momentum equation for solid phase m is

$$\frac{\partial \epsilon_{sm}\rho_{sm}\vec{\mathbf{u}}_{sm}}{\partial t} + \nabla \cdot (\epsilon_{sm}\rho_{sm}\vec{\mathbf{u}}_{sm}\vec{\mathbf{u}}_{sm}) = \nabla \cdot \bar{\bar{\mathbf{S}}}_{sm} + \vec{\mathbf{I}}_{gm} - \sum_{l=1, l\neq m}^{M} \vec{\mathbf{I}}_{ml} + \epsilon_{sm}\rho_{sm}\vec{\mathbf{g}} \tag{7}$$

where $\bar{\bar{\mathbf{S}}}_{sm}$ is the second-order stress tensor for the m^{th} solid phase, $\vec{\mathbf{I}}_{gm}$ is an interaction force representing the momentum transfer between the gas and the m^{th} solid phase, and Eq. (4) describes the momentum contribution due to solid-gas mass transfer. $\vec{\mathbf{I}}_{ml}$ is an interaction force representing the momentum transfer between the m^{th} and the l^{th} solid phases, and $\vec{\mathbf{g}}$ is the gravity vector.

The energy equation for the solid phases in terms of the m^{th} solid-phase temperature T_{sm} is

$$\epsilon_{sm}\rho_{sm}C_{psm} \left(\frac{\partial T_{sm}}{\partial t} + \vec{\mathbf{u}}_{sm} \cdot \nabla T_{sm} \right) = \nabla \cdot \vec{\mathbf{q}}_{sm} + \sum_{m=1}^{M} H_{gm} - \Delta H_{rsm} \tag{8}$$

where $\vec{\mathbf{q}}_{sm}$ is the m^{th} solid phase conductive heat flux, H_{gm} describes fluid-solids interphase heat transfer between the gas and m^{th} solids, and ΔH_{rsm} is the heat of reaction in the m^{th} solid phase. Radiative heat transfer is not considered in the current model.

The gas and solids phases may contain an arbitrary number of chemical species N. The species conservation equations considering the accumulation, convection, and rate of reaction for the gas phase is

$$\frac{\partial \epsilon_g \rho_g X_{gn}}{\partial t} + \nabla \cdot (\epsilon_g \rho_g X_{gn} \vec{\mathbf{u}}_g) = R_{gn} \tag{9}$$

where X_{gn} is the mass fraction and R_{gn} is the rate of formation of gas species n. R_{gn} can be found in Eq. (29). For consistency, $\sum_{n=1}^{N} R_{gn} = R_g$.

The species conservation equation for solid phase m is

$$\frac{\partial \epsilon_{sm}\rho_{sm}X_{smn}}{\partial t} + \nabla\cdot(\epsilon_{sm}\rho_{sm}X_{smn}\vec{\mathbf{u}}_{sm}) = R_{smn} \tag{10}$$

where X_{smn} is the mass fraction and R_{smn} is the rate of formation of solid phase m, species n. R_{smn} can be found in Eq. (30). For consistency, $\sum_{n=1}^{N} R_{smn} = R_{sm}$.

Kinetic theory is used in the derivation of the constitutive relation describing the stress tensor in the m^{th} solid phase, $\bar{\bar{\mathbf{S}}}$. A granular temperature Θ_m is defined for each solid phase, and it is described as the specific kinetic energy of the random fluctuating component of the particle velocity:

$$E_{\Theta_m} = \frac{3}{2}\Theta_m \tag{11}$$

where E_{Θ_m} is the granular energy. The transport of the mixture granular energy Θ can be solved and then the granular temperature for the m^{th} solid phase can be obtained. Here, an algebraic expression for granular temperature Θ_m is calculated (Syamlal et al., 1993).

A Newtonian closure is used for the gas-phase stress tensor. Two different methods are used to calculate the solid stress tensor in the plastic and viscous regimes (Syamlal et al., 1993; Gidaspow, 1994; Lun et al., 1984). The gas-solid drag correlation was derived by Syamlal et al. (1993). The interaction forces between the different solid phases are expressed in terms of the drag force and the enduring contact force in the plastic regime, as described in Syamlal et al. (1993). The heat transfer between gas and solids is assumed to be a function of the temperature difference. Conductive heat flux in the fluid phase is governed by Fourier's Law. Conductive heat flux for the solid phases is assumed to have a similar form to that in the fluid phase (Syamlal and Gidaspow, 1985). A detailed discussion of these parameters in the multi-fluid CFD model can be found elsewhere (Syamlal et al., 1993). The mass-transfer parameters are related to chemical kinetics as described in Eqs. (29,30).

2.3 Numerical algorithm of coupling kinetics and hydrodynamics

The coupling of hydrodynamics of gas-solid flow and chemical reaction of biomass is achieved using a time-splitting approach (Xie et al., 2004; Pope, 1997), which calculates the transport and source terms separately at each time-step. The decoupled calculation procedure of transport and reaction sources is shown in Eq. (12). At each time step, the solution is first advanced to an intermediate value $\phi^*(t+\Delta t)$ due to transport fluxes from initial value $\phi(t)$ at time t. Then the intermediate value $\phi^*(t+\Delta t)$ is updated to $\phi(t+\Delta t)$ at time $t+\Delta t$ by taking account for reactions:

$$\phi(t) \xrightarrow{\text{Convection + Diffusion}} \phi^*(t+\Delta t) \xrightarrow{\text{Reactions}} \phi(t+\Delta t) \tag{12}$$

Within the time-splitting approach, the conservation equations solved in the CFD solver are rewritten as follows. First, the following set of equations with $M = 2$ solid phases (sand and biomass) is solved to obtain the solution $\phi^*(t+\Delta t)$ from the initial values $\phi(t)$:
Gas continuity:

$$\frac{\partial}{\partial t}(\epsilon_g\rho_g) + \nabla\cdot(\epsilon_g\rho_g\vec{v}_g) = 0, \tag{13}$$

Gas species:

$$\frac{\partial}{\partial t}(\epsilon_g\rho_g X_{gn}) + \nabla\cdot(\epsilon_g\rho_g X_{gn}\vec{v}_g) = \nabla\cdot D_{gn}\nabla X_{gn}, \tag{14}$$

Solid continuity:

$$\frac{\partial}{\partial t}(\epsilon_{sm}\rho_{sm}) + \nabla\cdot(\epsilon_{sm}\rho_{sm}\vec{v}_{sm}) = 0, \tag{15}$$

Solid species:

$$\frac{\partial}{\partial t}(\epsilon_{sm}\rho_{sm}X_{smn}) + \nabla\cdot(\epsilon_{sm}\rho_{sm}X_{smn}\vec{v}_{sm}) = 0, \tag{16}$$

Gas momentum:

$$\frac{\partial \epsilon_g \rho_g \vec{\mathbf{u}}_g}{\partial t} + \nabla \cdot (\epsilon_g \rho_g \vec{\mathbf{u}}_g \vec{\mathbf{u}}_g) = \nabla \cdot \bar{\bar{\mathbf{S}}}_g + \sum_{m=1}^{M} \vec{\mathbf{I}}_{gm} + \epsilon_g \rho_g \vec{\mathbf{g}}, \tag{17}$$

Solid momentum:

$$\frac{\partial \epsilon_{sm} \rho_{sm} \vec{\mathbf{u}}_{sm}}{\partial t} + \nabla \cdot (\epsilon_{sm} \rho_{sm} \vec{\mathbf{u}}_{sm} \vec{\mathbf{u}}_{sm}) = \nabla \cdot \bar{\bar{\mathbf{S}}}_{sm} + \vec{\mathbf{I}}_{gm} - \sum_{l=1, l\neq m}^{M} \vec{\mathbf{I}}_{ml} + \epsilon_{sm} \rho_{sm} \vec{\mathbf{g}}, \tag{18}$$

Gas energy:

$$\epsilon_g \rho_g C_{pg} \left(\frac{\partial T_g}{\partial t} + \vec{v}_g \cdot \nabla T_g \right) = -\nabla \cdot \vec{q}_g + \sum_{m=1}^{M} \gamma_{gm} (T_{sm} - T_g), \tag{19}$$

Solid energy:

$$\epsilon_{sm} \rho_{sm} C_{psm} \left(\frac{\partial T_{sm}}{\partial t} + \vec{v}_{sm} \cdot \nabla T_{sm} \right) = -\nabla \cdot \vec{q}_{sm} - \sum_{m=1}^{M} \gamma_{gm} (T_{sm} - T_g). \tag{20}$$

Note that the species equations are solved only for the non-zero values of X_n for each phase. The solutions of Eqs. (13)-(20) are $\phi^*(t + \Delta t)$, which serve as the initial values for the chemical reaction step.

An implicit ordinary differential equation (ODE) solver (Hindmarsh, 1983) for stiff ODEs is applied to solve the set of initial-value problems for the chemical reactions. During the reaction step, the phase volume fractions (ϵ_g, ϵ_{s1}, ϵ_{s2}) are constant. The equations of change due to chemical reactions in a finite-volume cell are written as follows.

Gas mass balance:

$$\frac{d\rho_g}{dt} = -\frac{1}{\epsilon_g} \sum_{n=1}^{N} R_{s2,n}, \tag{21}$$

Gas species mass balance:

$$\frac{dX_{gn}}{dt} = \frac{1}{\rho_g \epsilon_g} \left[R_{gn} + X_{gn} \sum_{l=1}^{N} R_{s2,l} \right], \tag{22}$$

Solid mass balance:

$$\frac{d\rho_{s2}}{dt} = \frac{1}{\epsilon_{s2}} \sum_{n=1}^{N} R_{s2,n}, \tag{23}$$

Solid species mass balance:

$$\frac{dX_{s2,n}}{dt} = \frac{1}{\rho_{s2} \epsilon_{s2}} \left[R_{s2,n} - X_{s2,n} \sum_{l=1}^{N} R_{s2,l} \right], \tag{24}$$

Gas energy balance:

$$\frac{dT_g}{dt} = -\frac{\Delta H_{rg}}{\rho_g \epsilon_g C_{pg}}, \tag{25}$$

Solid energy balance:

$$\frac{dT_{s2}}{dt} = -\frac{\Delta H_{rs2}}{\rho_{s2} \epsilon_{s2} C_{ps2}}. \tag{26}$$

During the simulation, these equations are integrated repetitively for each cell at every time step with each new set of initial conditions $\phi^*(t+\Delta t)$. The chemical source terms (R) on the right-hand sides of these equations are defined in Eqs. (29, 30). The source for the gas mass balance Eq. (21) is attributed to the mass transfer from the biomass phase due to chemical reactions in solid phase $s2$. The heats of reaction are included in the energy balance in terms of temperature. The heat of reactions are

accordingly assigned to the solid phase in Eq. (26) and the gas phase in Eq. (25), respectively. With initial values from the solution of Eqs. (13)-(20), Eqs. (21)-(26) can be solved by integration over one time step for every computational volume, and thus solutions are update to $\phi(t + \Delta t)$. With the new values of density and temperature, the gas-phase pressure is then updated using the equation of state for an ideal gas. The solution completes one time-step and advances to the next time-step. Note that the momentum transfer is included in the term $\vec{I}_{gm}$ of the momentum equation Eq. (17) and Eq. (18). In the meantime, the momentum transfer due to the reaction is updated in the transport calculation step, which is suitable for the numerical algorithm based on a staggered grid.

2.4 Variable particle density model and uniform conversion model

One of the keys for our successful implementation is to account for the variable biomass apparent density due to reaction and convection. The hydrodynamics of the multiphase flow system strongly depend on the density of the particles in each solid phase. The hydrodynamics of biomass particles directly influence the particle residence time through the terminal velocity in the reactor, and thus impacts on the conversion efficiency and char elutriation. It is critical to predict the particle density variation for gasifier simulations. Very light particles, for example, tend to segregate and elutriate from the reactor by the carrier gas, while heavier particles are more difficult to fluidize. Due to the conversion of the solid biomass phase to gas products, the density of biomass particles decreases as the reaction progresses assuming the biomass particle diameter remains constant. Hence, the biomass phase consists of freshly fed biomass, partially converted, and fully converted nonreacting particles, simultaneously. To account for this spatial-temporal property, the transport equation Eq. (6) is solved for the mean particle mass with varying apparent density for the reacting biomass phase. In this model, the apparent density is updated through knowledge of the mass and porosity of the particle phase, which can be related to the particle mass, control volume, and biomass phase composition. In a finite-volume framework, the biomass apparent density is updated due to transport using

$$\frac{1}{\rho_{apparent}} = \sum_{n=1}^{N} \frac{X_{s_2 n}}{(\rho_n)_{true}} \tag{27}$$

where $(\rho_n)_{true}$ is the true density of species n that is constant. $X_{s_2 n}$ is mass fraction of species n and is solved through species balance equation (Eq. (10)).

Here, a uniform conversion model is adopted to represent the particle reaction for particle size less than 1 mm. The model does not consider the diffusion and concentration gradient inside the particle, and thus describes a constant particle size with a variable particle density. Other conversion models for coal gasification can be extended to biomass, particularly for large particles, and can be found elsewhere (Gomez-Barea and Leckner, 2010).

2.5 Chemical kinetic source terms for reactive biomass phase

In the multi-fluid CFD approach, instead of considering individual particles, the particles are treated as a continuous phase. For this purpose, first-order expressions of the chemical kinetics for each species are formulated in a finite volume. The source terms are written as in Eq. (28). In the lumped kinetic scheme for micro-particles, we assume that there is no gradient in concentration inside the particle and the chemistry does not depend on product concentrations. Thus, there is no mass-transfer limitation. The mass transfer rate to gas depends on the reaction rate. The particle temperature is assumed to be uniform inside the particle due to its small size, which implicitly assumes very small Biot numbers for the particles. The resistance to heat transfer for particles is mainly at the gas-solid interface, which is calculated through the Nusselt correlation (Gunn, 1978; Syamlal et al., 1993).

$$\frac{dm}{dt} = -km \tag{28}$$

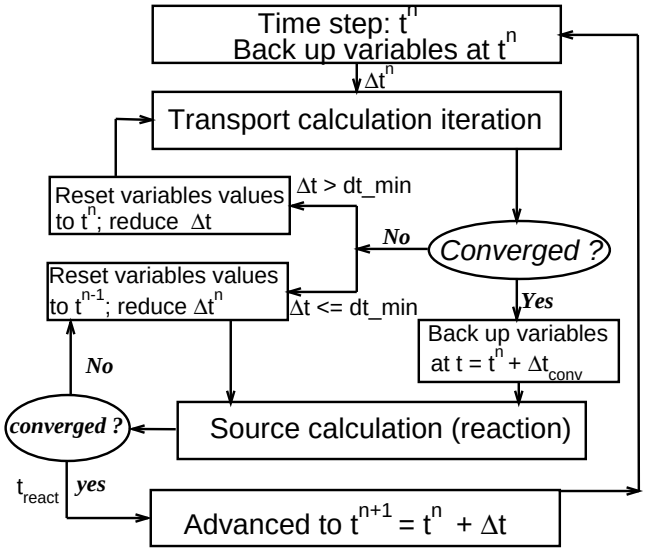

Figure 1: Flow chart of CFD calculations of biomass gasification in a multi-fluid CFD model with solution restart for strong chemistry over one complete time-step from t^n to t^{n+1}.

When the mass of biomass species and temperature for the reaction rate are obtained using the mean values of the gas phase and biomass phase in a computational cell, it can be used to formulate the chemical reaction source terms $R_{s_m n}$ and R_{g_n} that arise in the multi-fluid CFD model. Eqs. (29) and (30) show the first-order forms for R_{g_n} and $R_{s_m n}$ written in terms of the kinetic parameters and mean values in a finite-volume cell. The phase indices of the gas phase, the sand phase, and the biomass phase are g, s_1, and s_2, respectively. X_{s_2} and X_g are the mass fractions of biomass species and gas species, respectively. Note that the sand phase (s_1) is inert and hence all reaction rates $R_{s_1 n}$ are null.

$$R_{gn} = -\rho_g \epsilon_{gn} X_{gn} k_{gn} \quad (29)$$

$$R_{s2,n} = -\rho_{s2} \epsilon_{s2,n} X_{s2,n} k_{s2,n} \quad (30)$$

2.6 Numerical solution procedure for gas-particle reactive flows

MFIX is a pressure-based fluid-solids flow solver (Syamlal et al., 1993; Syamlal, 1998). The governing equations (Eqs. (2)–(10)) are spatially discretized using a finite-volume technique on a staggered grid. Convective fluxes are approximated with a second-order accurate bounded TVD-scheme avoiding the excessive numerical diffusion associated with the first-order accurate upwind scheme. The semi-implicit SIMPLE algorithm is applied to solve the system of equations. An effective partial elimination algorithm (PEA) is applied for interphase coupling. An automatic time-step adjustment is used to reduce the run time. A combination of linear equation solvers is used to solve the system of under-relaxed discretized equations. The calculation procedure for coupling transport and reaction source terms is in a time-splitting approach (Pope, 1997; Xie et al., 2004) (as shown in Figure 1). A convection-diffusion calculation is performed in the first fractional time. Time integration of the equations is then performed with only the reaction source terms present for every computational cell. The advantages of this split scheme are that standard convection-diffusion systems are easily handled within the hydrodynamics, whereas there is no spatial coupling in the second fractional step. The stiff integration of the system of ODEs in the second step is performed using the ODE solver ODEPACK (LSODA Fortran double-precision subroutine) (Hindmarsh, 1983). As can be seen in Figure 1, a time-step adaption and restart procedure was implemented to provide the stability for strong chemical reaction in the time-splitting approach. Which is achieved by a parameter in the

Table 1: Key parameters for variable particle density model.

Keywords (dimension)	**Type**	**Description**
SOLID_RO_V [.FALSE.]	L	Indicate if the variable particle density model activated or not
RO_SV(:,m)	DP	Filed particle density
RO_SS(m,NMAX(m))	DP	Species density
RESTART_REACTION [.FALSE.]	L	Control restart iteration from previous time with a reduced time-step, when solver cannot converge due to strong chemical source term

code (RESTART_REACTION). In the transient process, a synchronized time-step uses the minimum value of the time-step for transport and that for reaction for the sake of accuracy and stability of the CFD code in our current implementation. It is worth to mention that with the improved solution procedure, the standard relaxation factors (Syamlal, 1998; Patankar, 1980) for the SIMPLE algorithm are allowed to simulate the biomass gasifier with strong mass and heat transfer. This is important for achieving numerical solution efficiency for reactive flow simulations in energy reactors such as gasifier.

3 Tutorials

3.1 Key parameters

The key parameters for variable particle density model implementation and case setup are listed in Table 1.

3.2 Input control and variable parameters

Here are the necessary parameters that have to be provided in input file (mfix.dat) for using variable particle density model. The description of all these parameters can be found in MFIX Readme file.

1. To activate the variable particle density model in the solver,
   - SOLID_RO_V = .TRUE.
2. Provide true density for solid species (for example, solid phase 2, with NMAX(2) number of species),
   - RO_SS(2,1) = density of species one
   - RO_SS(2,2) = density of species two
   - .....
   - RO_SS(2,NMAX(2)) = density of species NMAX(2)
3. To use the direct integration solver for the chemistry,
   - CALL_DI = .TRUE.

3.3 Example case: biomass devolatilization

Here is the input mfix.dat file for biomass devolatilization in a fluidized-bed reactor. This test case should be available with the MFIX-varaible particle density release.

```
! Run-control section
  RUN_NAME                  = 'bio'
  DESCRIPTION               = 'devol'
  RUN_TYPE                  = 'NEW'
  UNITS                     = 'cgs'
  TIME                      = 0.0                   !start
  TSTOP                     = 20.0
  DT                        = 1.0E-06               !time-step
  DT_MIN                    = 1.0D-08
  DT_MAX                    = 1.0E-03
  DETECT_STALL              = .FALSE.
  CLOSE_PACKED              = .TRUE.      .TRUE.
  ENERGY_EQ                 = .TRUE.
  SPECIES_EQ                = .TRUE.      .FALSE.     .TRUE.
  DISCRETIZE                = 7*2
  MAX_NIT                   = 50
  CALL_USR   = .TRUE.
  CALL_DI    = .TRUE.

  SOLID_RO_V = .TRUE.

! Geometry section

  COORDINATES    = 'cartesian'
  XLENGTH        =   4.0
  IMAX           =   10
  YLENGTH        =   28.0
  JMAX           =   70
  NO_K           = .TRUE.                          !2D, no k direction
  SEGREGATION_SLOPE_COEFFICIENT     = 0.3
  ep_s_max(1)                       = 0.6
  ep_s_max(2)                       = 0.6
  FEDORS_LANDEL = .TRUE.

! Gas-phase section

  MU_g0                     = 3.491E-4
  NMAX(0)                   = 9
  Mw_g = 32.0 28.0 18.0 28.0 44.0 2.0 16.0 100.0 100.0

! Solids-phase section

  MMAX                      = 2
  RO_s                      = 2.649d0    0.585d0      !density
  D_p0                      = 0.052d0    0.05d0       !diameter
  NMAX(1)                   = 1
  NMAX(2)                   = 5
  RO_SS(2,1)                = 0.585d0
  RO_SS(2,2)                = 0.649d0
  RO_SS(2,3)                = 0.450d0
  RO_SS(2,4)                = 4.2110d-4
  RO_SS(2,5)                = 0.450d0
  e                         = 0.97d0                !restitution coefficient
  C_f                       = 0.1d0
  Phi                       = 30.d0
  EP_star                   = 0.4d0

! Initial conditions section

    ! 1. bed
  IC_X_w(1)                 =  0.0
  IC_X_e(1)                 =  4.0
  IC_Y_s(1)                 =  0.0
  IC_Y_n(1)                 =  8.0
  IC_EP_g(1)                =  0.395d0              !void fraction
  IC_X_g(1,1)               =  0.0
  IC_X_g(1,2)               =  1.0
  IC_X_g(1,3)               =  0.0
  IC_X_g(1,4)               =  0.0
  IC_X_g(1,5)               =  0.0
  IC_X_g(1,6)               =  0.0
  IC_X_g(1,7)               =  0.0
  IC_X_g(1,8)               =  0.0
```

```
  IC_X_g(1,9)             =  0.0
  IC_ROP_s(1,1)           =  1.602645d0
  IC_X_s(1,1,1)           =  1.0
  IC_ROP_s(1,2)           =  0.0
  IC_X_s(1,2,1)           =  1.0
  IC_X_s(1,2,2)           =  0.0
  IC_X_s(1,2,3)           =  0.0
  IC_X_s(1,2,4)           =  0.0
  IC_X_s(1,2,5)           =  0.0
  IC_U_g(1)               =  0.0
  IC_V_g(1)               =  0.0
  IC_U_s(1,1)             =  0.0
  IC_V_s(1,1)             =  0.0
  IC_U_s(1,2)             =  0.0
  IC_V_s(1,2)             =  0.0
  IC_T_g(1)               =  973.0
  IC_T_s(1,1)             =  973.0
  IC_T_s(1,2)             =  973.0
  IC_P_g(1)               =  1.01E6
  IC_P_star(1)            =  0.0
    !  2. Freeboard
  IC_X_w(2)               =  0.0
  IC_X_e(2)               =  4.0
  IC_Y_s(2)               =  8.0
  IC_Y_n(2)               =  28.0
  IC_EP_g(2)              =  1.0
  IC_X_g(2,1)             =  0.0
  IC_X_g(2,2)             =  1.0
  IC_X_g(2,3)             =  0.0
  IC_X_g(2,4)             =  0.0
  IC_X_g(2,5)             =  0.0
  IC_X_g(2,6)             =  0.0
  IC_X_g(2,7)             =  0.0
  IC_X_g(2,8)             =  0.0
  IC_X_g(2,9)             =  0.0
  IC_ROP_s(2,1)           =  0.0
  IC_ROP_s(2,2)           =  0.0
  IC_U_g(2)               =  0.0
  IC_V_g(2)               =  0.0
  IC_U_s(2,1)             =  0.0
  IC_V_s(2,1)             =  0.0
  IC_U_s(2,2)             =  0.0
  IC_V_s(2,2)             =  0.0
  IC_T_g(2)               =  973.0
  IC_T_s(2,1)             =  973.0
  IC_T_s(2,2)             =  973.0
  IC_P_g(2)               =  1.01E6
  IC_P_star(2)            =  0.0

!  Boundary conditions section

      ! 1. Distributor jet
  BC_X_w(1)               =  0.0
  BC_X_e(1)               =  4.0
  BC_Y_s(1)               =  0.0
  BC_Y_n(1)               =  0.0
  BC_TYPE(1)              =  'MI'          !mass inflow
  BC_EP_g(1)              =  1.0
  BC_X_g(1,1)             =  0.24
  BC_X_g(1,2)             =  0.76
  BC_X_g(1,3)             =  0.0
  BC_X_g(1,4)             =  0.0
  BC_X_g(1,5)             =  0.0
  BC_X_g(1,6)             =  0.0
  BC_X_g(1,7)             =  0.0
  BC_X_g(1,8)             =  0.0
  BC_X_g(1,9)             =  0.0
  BC_U_g(1)               =  0.0
  BC_V_g(1)               =  23.7
  BC_P_g(1)               =  1.01d+6
  BC_T_g(1)               =  673.0

      ! 2. Biomass injection
```

```
  BC_X_w(2)              = 0.0
  BC_X_e(2)              = 0.0
  BC_Y_s(2)              = 1.2
  BC_Y_n(2)              = 2.0
  BC_TYPE(2)             = 'MI'
  BC_EP_g(2)             = 0.993022
  BC_P_g(2)              = 1.01d+6
  BC_ROP_s(2,1)          = 0.0
  BC_ROP_s(2,2)          = 0.00408213
  BC_T_g(2)              = 300.0
  BC_T_s(2,1)            = 300
  BC_T_s(2,2)            = 300
  BC_U_g(2)              = 12.357
  BC_V_g(2)              = 0.0
  BC_U_s(2,2)            = 12.357
  BC_V_s(2,2)            = 0.0
  BC_X_g(2,1)            = 0.0
  BC_X_g(2,2)            = 1.0
  BC_X_g(2,3)            = 0.0
  BC_X_g(2,4)            = 0.0
  BC_X_g(2,5)            = 0.0
  BC_X_g(2,6)            = 0.0
  BC_X_g(2,7)            = 0.0
  BC_X_g(2,8)            = 0.0
  BC_X_g(2,9)            = 0.0
  BC_X_s(2,2,1)          = 1.0
  BC_X_s(2,2,2)          = 0.0
  BC_X_s(2,2,3)          = 0.0
  BC_X_s(2,2,4)          = 0.0
  BC_X_s(2,2,5)          = 0.0

       ! 2. Exit
  BC_X_w(3)              = 0.0
  BC_X_e(3)              = 4.0
  BC_Y_s(3)              = 28.0
  BC_Y_n(3)              = 28.0
  BC_TYPE(3)             = 'PO'          !pressure outflow
  BC_P_g(3)              = 1.01d+6
  BC_T_g(3)              = 973.0

!  Output Control

  OUT_DT                 = 10.           !write text file .OUT
  RES_DT                 = 0.1           !write binary restart file
  NLOG                   = 25            !write logfile .LOG
  FULL_LOG               = .TRUE.        !display residuals on screen

  !SPX_DT values determine how often SPx files are written.
  SPX_DT = 0.1 0.1 0.1 0.1 0.1 0.1 0.1 0.1 0.1
  RESID_STRING  = 'P0' 'R1' 'U0' 'R2' 'V0' 'V1' 'V2'

  !The domain decomposition for DMP
  NODESI = 1   NODESJ = 1   NODESK = 1
```

References

M. Syamlal, W. Rogers, T. J. O'Brien, MFIX documentation: theory guide, Technical Note DOE/METC-95/1013, U. S. Department of Energy, 1993.

M. Syamlal, MFIX documentation: numerical technique, Technical Note DOE/MC31346-5824, U. S. Department of Energy, 1998.

Q. Xue, T. J. Heindel, R. O. Fox, A CFD model for biomass fast pyrolysis in fluidized-bed reactors, Chemical Engineering Science 66 (2011) 2440–2452.

Q. Xue, D. Dalluge, T. J. Heindel, R. O. Fox, R. C. Brown, Experimental validation and CFD modeling study of biomass fast pyrolysis in fluidized-bed reactors, Fuel 97 (2012) 757–769.

Q. Xue, R. O. Fox, An Euler-Euler CFD model for biomass gasification in fluidized beds, in: NETL 2012 Conference on Multiphase Flow Science, Morgantown, WV.

Q. Xue, R. O. Fox, Multi-fluid CFD modeling of biomass gasification in polydisperse fluidized-bed gasifiers, (under review) (2013).

D. Gidaspow, Multiphase flow and fluidization, Academic Press, 1994.

C. Lun, S. Savage, D. Jeffrey, N. Chepurniy, Kinetics theories for granular flow: inelastic particles in couette flow and slightly inelastic particles in a general flowfield, Journal of Fluid Mechanics 223 (1984) 140.

M. Syamlal, D. Gidaspow, Hydrodynamics of fluidization: prediction of wall to bed heat transfer coefficients, AIChE Journal 31 (1985) 127–135.

N. Xie, F. Battaglia, R. O. Fox, Simulation of multiphase reactive flows in fluidized beds using *in situ* adaptive tabulation, Combustion Theory and Modelling 8 (2004) 195–209.

S. B. Pope, Computationally efficient implementation of combustion chemistry using in situ adaptive tabulation, Combustion Theory and Modelling 1 (1997) 41–63.

A. C. Hindmarsh, ODEPACK, a systemized collection of ODE solvers, in: Scientific computing, Amsterdam: North-Holland, 1983.

A. Gomez-Barea, B. Leckner, Modeling of biomass gasification in fluidized bed, Progress in Energy and Combustion Science 36 (2010) 444–509.

D. J. Gunn, Transfer of heat or mass to particles in fixed and fluidized beds, International Journal of Heat Mass Transfer 21 (1978) 467–476.

S. V. Patankar, Numerical heat transfer and fluid flow, Taylor & Francis, 1980.